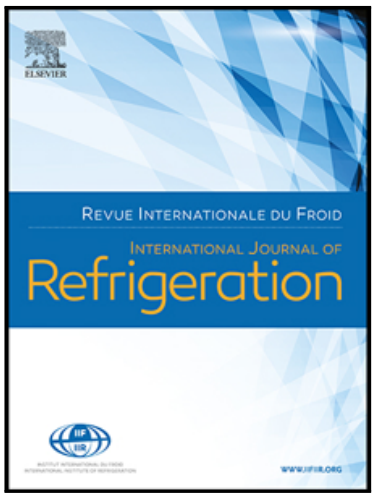

Theoretical performance evaluation of ejector and economizer with parallel compression configurations in high temperature heat pumps

Carlos Mateu-Royo , Joaquín Navarro-Esbrí ,
Adrián Mota-Babiloni , Ángel Barragán-Cervera

PII: S0140-7007(20)30318-2
DOI: https://doi.org/10.1016/j.ijrefrig.2020.07.016
Reference: JIJR 4845

To appear in: *International Journal of Refrigeration*

Received date: 23 March 2020
Revised date: 16 June 2020
Accepted date: 22 July 2020

Please cite this article as: Carlos Mateu-Royo , Joaquín Navarro-Esbrí , Adrián Mota-Babiloni , Ángel Barragán-Cervera , Theoretical performance evaluation of ejector and economizer with parallel compression configurations in high temperature heat pumps, *International Journal of Refrigeration* (2020), doi: https://doi.org/10.1016/j.ijrefrig.2020.07.016

Highlights

- Ejector and parallel compression configurations are proposed for high temperature heat pumps.
- Internal heat exchanger analysis is included in the proposed configurations.
- Alternative sustainable refrigerant assessment is performed to replace HFC-245fa.
- Multi-objective analysis evaluates the compromise between volumetric heating capacity and COP.
- Advanced high temperature heat pump configurations are promoted.

Theoretical performance evaluation of ejector and economizer with parallel compression configurations in high temperature heat pumps

Carlos Mateu-Royo[a*], Joaquín Navarro-Esbrí[a], Adrián Mota-Babiloni[a], Ángel Barragán-Cervera[a]

[a]ISTENER Research Group, Department of Mechanical Engineering and Construction, Universitat Jaume I, Campus de Riu Sec s/n, E12071 Castelló de la Plana, Spain

Abstract

Climate change evolution urges us to take action to reduce greenhouse gas emissions. As one of the main contributors, the industrial sector requires cleaner methods of heat production, such as high temperature heat pumps (HTHP) with the highest energy efficiency. Facing this challenge, this paper provides a performance comparison of the ejector and parallel compression configurations in HTHPs for low-grade waste heat recovery. A single-stage cycle has been used as a reference configuration to compare the proposed options. The internal heat exchanger (IHX) is included in all the configurations to extend the analysis and illustrate the influence of this component in high temperature applications. Moreover, alternative low-GWP (global warming potential) refrigerants have been analyzed in order to replace the reference working fluid HFC-245fa. Ejector and parallel compression configurations with IHX provide a coefficient of performance (COP) improvement of up to 36% and 72.5%, respectively, using HFC-245fa for a heating temperature production of 140 ºC. Moreover, the volumetric heating capacity (VHC) increases around 36% for the ejector cycle and 80% for the parallel compression cycle with IHX. HC-601, HFO-1336mzz(Z), and R-514 have the most significant COP improvement compared to HFC-245fa, along with the highest VHC drop. Multi-objective evaluation illustrates that single-stage and ejector configurations with IHX have similar results, whereas the parallel compression cycle with IHX presents a significant COP and VHC improvement. HCFO-1233zd(E) and HCFO-1224yd(Z) presents the proper trade-off between COP and VHC.

Keywords: waste heat revalorization; advanced configurations; liquid-to-suction heat exchanger (LSHX); low GWP refrigerants; energy efficiency; HTHP.

Nomenclature

a, b, k_e, k_s, k_1, k_2	Pierre's correlations constants
COP	coefficient of performance (-)
h	specific enthalpy (kJ kg^{-1})
$\dot{m}$	refrigerant mass flow rate (kg s^{-1})
P	pressure (MPa)
$\dot{Q}$	thermal loads (kW)
T	temperature (ºC)
SC	sub-cooling degree (K)
SH	superheat degree (K)
$\dot{W}$	electric power consumption (kW)
VHC	volumetric heating capacity (kJ m^{-3})

* Corresponding author: Carlos Mateu-Royo
Tel: +34 964 728 134
Email: mateuc@uji.es

Greek symbols

ε	effectiveness (-)
η	efficiency (-)
Δ	variation
ρ	density (kg m^{-3})

Subscripts

c	compressor
crit	critical
disch	compressor discharge temperature
em	electromechanical
in	inlet
iso	isentropic
k	condenser
o	evaporator
out	outlet
ref	reference configuration or working fluid
sat	saturated
sink	heat sink
source	heat source
suc	suction
vap	vapour
vol	volumetric

Abbreviations

EES	engineering equation solver
GWP	global warming potential
HC	hydrocarbon
HCFO	hydrochlorofluoroolefin
HFC	hydrofluorocarbon
HFO	hydrofluoroolefin
HTHP	high temperature heat pump
IHX	internal heat exchanger
Ref	reference

1. Introduction

High temperature heat pumps (HTHPs) are an excellent alternative to replace natural gas boilers in the coming years, especially in scenarios that consider an economy moving towards a higher penetration of renewable energy technologies (Bergamini et al., 2019). Kosmadakis (2019) estimated that the necessary annual waste heat recovery with heat pump technology in the EU industries is approximately 21 TWh, which corresponds to 7% of the total potential waste heat. They indicated that the non-metallic minerals, food, paper, and non-ferrous metal industries are the most promising industries for applying this technology. These predictions are in agreement with Cooper et al. (2019), who indicate that a potential amount of 2.6 $MTCO_2$ can annually save in the food and drink sector (considering 2030 carbon emission electricity factors). On the other hand, HTHPs, as flexible systems, can cover variable energy demand, achieving valuable economic and energy savings and, therefore, becoming a promising technology for trigeneration systems (Urbanucci et al., 2019).

Arpagaus et al. (2018) published a comprehensive review that covered different aspects of the current situation of HTHPs. They proved that this technology could adapt to various industrial applications, heat sink and source temperatures, and heating capacities, given the variety of

possibilities that offers the selection of components construction, working fluids, and configurations. Mateu-Royo et al. (2019b) use a novel HTHP with a modified scroll compressor and HFC-245 to achieve a heat sink temperature of 140 °C with a coefficient of performance (COP) of 2.23. Arpagaus et al. (2019) measured the performance of the working fluids HCFO-1233zd(E), HCFO-1224yd(Z), and HFO-1336mzz(Z), obtaining a COP of 3.1, 3.0, and 2.8, respectively.

From a theoretical perspective, the single-stage cycle with IHX is beneficial for moderate-high temperature applications with low-temperature lift (Mateu-Royo et al., 2018). For high temperature lift, a two-stage cycle with IHX achieves an apparent COP increase. A similar situation is observed by Mota-Babiloni et al. (2018) with optimized two-stage cascades, which energy benefit only results evident above 60 K. Arpagaus et al. (2019b) investigated several two-stage cycles (economizer, flash tank, and cascade) theoretically and concluded that depending on the refrigerant and cycle, a trade-off between system complexity (e.g. control, number of components), efficiency, and volumetric heating capacity (VHC) has to be found. Optimal COPs were reached depending on the refrigerant and its heat outlet temperature. A two-stage cascade with IHX and HFO-1336mzz(Z) in both stages achieved the highest efficiency for high temperature lifts. The use of an IHX in the cycle was recommended to ensure dry compression; a two-stage cascade cycle for high temperature lifts of 70 K and higher. Fang et al. (2019) realized a study of a modified refrigeration cycle with parallel compression for refrigeration applications, using HC-290/HC-600a as a mixture to replace HFC-134a.

Arpagaus et al. (2016) have theoretically studied and compared from an energetic and exergetic point of view several configurations. After multi-stage cycles, the parallel compressor architecture results in higher first and second law efficiency. Then, the ejector expansion cycle seems to be promising for system performance improvement. Bai et al. (2019) studied the two ejector configurations that ended with an energy increase compared to the basic configuration. Besides, Luo and Zou (2019) found more benefits in terms of heating production with several ejector combinations. The review paper of Zhang et al. (2020) showed the operational and energetic benefits of ejector-expansion technology in vapor compression systems. Nevertheless, most of the theoretical studies that consider ejectors for refrigerant applications and using CO_2 as working fluid (Pérez-García et al., 2016; Rodríguez-Muñoz et al., 2018). The same situation exists with parallel compression (Mohammadi and Powell, 2020; Sun et al., 2020). Nevertheless, these configurations are not comprehensive analysed in heat pumps for high temperature applications, using different low GWP refrigerants.

Based on the above discussed, ejector and parallel compression configurations are promising architectures that can end in energetic benefits for HTHPs as alternative to single-stage cycle for low temperature lift applications. This paper aims to provide a complete analysis of these configurations, covering a wide range of operating temperatures and low GWP working fluids. Moreover, IHX is included to extend the study of the configurations. Finally, multi-objective evaluation is realized to provide the most balanced configuration and low-GWP refrigerant from VHC and COP point of view.

2. System configurations

2.1 Single-stage cycle

The schematic of a standard single-stage cycle with an internal heat exchanger (IHX) and its P-h diagram is shown in Fig.1. This system has become the reference configuration in high temperature heat pump technology. It is composed of the four main components in the vapor compression cycle: compressor, condenser, expansion valve, and evaporator together with an IHX between the suction and the liquid lines. This additional heat exchanger increases the sub-cooling and superheating degree, transferring heat internally from the condenser outlet to the compressor suction.

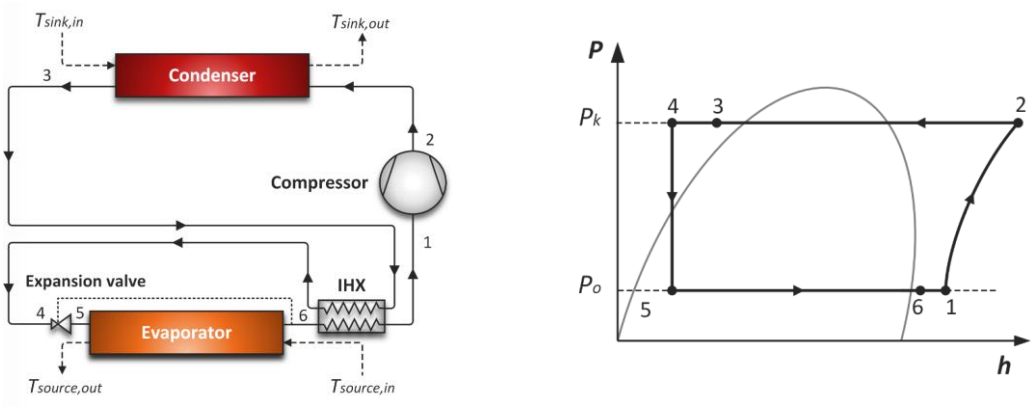

(a) (b)

Fig. 1. Single-stage configuration with IHX: a) Schematic and b) P-h diagram.

2.2 Economizer with parallel compression cycle

Single-stage configuration can be modified with the addition of an economizer and parallel compressor to obtain an advanced configuration, as shown in Fig. 2. The economizer is a type of sub-cooler where part of the refrigerant, typically 10-20% (Tello-Oquendo et al., 2019), is evaporated at a higher evaporation temperature than in the main evaporator while subcooling the remaining refrigerant flow substantially (SWEP). The extracted liquid fraction evaporates with a certain superheat degree, and it is compressed from an intermediate pressure level by the parallel compressor. The economizer increases the sub-cooling degree allowing it to absorb more heat in the evaporator. The total sub-cooling is increased then by keeping the IHX between the economizer outlet and the suction line.

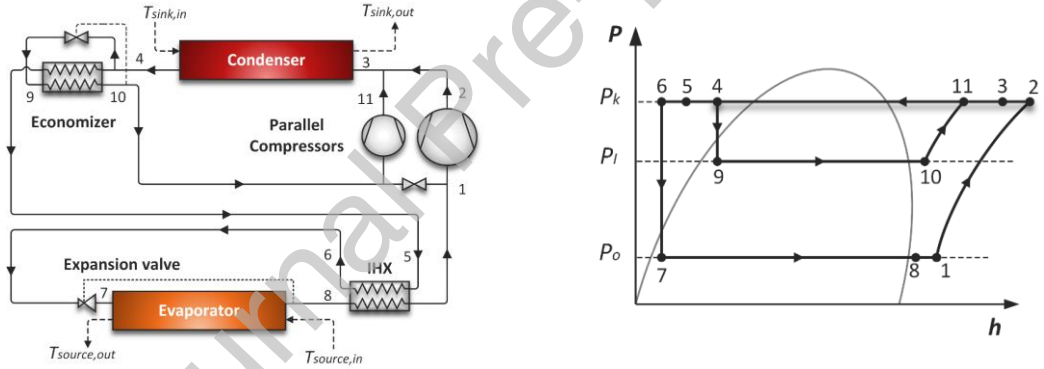

(a) (b)

Fig. 2. Economizer with parallel compression configuration with IHX: a) Schematic and b) P-h diagram.

2.3 Ejector cycle

The ejector can be implemented in a single-stage cycle along with IHX to obtain an advanced configuration, as shown in Fig. 3. Although there are several ejector configurations (Zhang et al., 2020), it has been selected the configuration with an IHX to maximize the discharge temperature. Moreover, this configuration requires the addition of a liquid receiver to ensure proper operation.

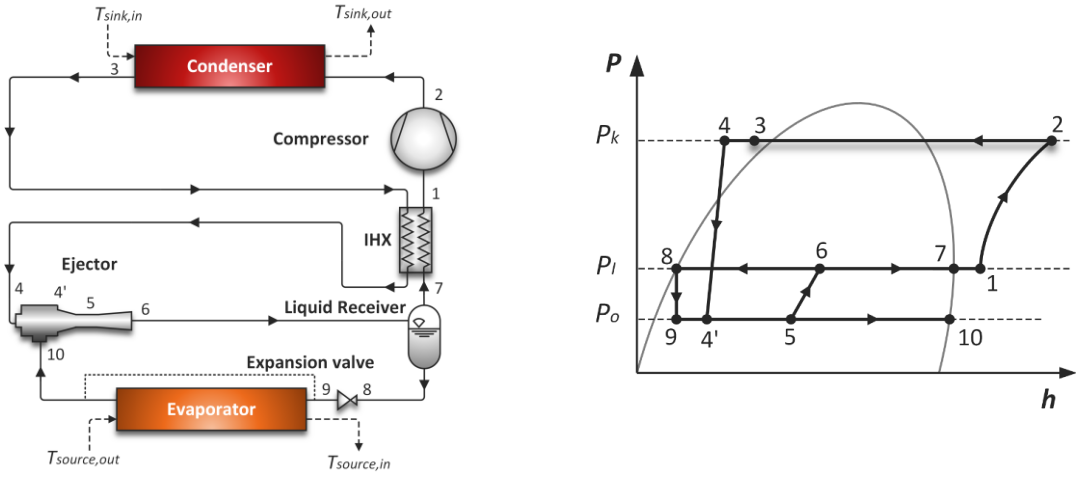

(a) (b)

Fig. 3. Ejector configuration with IHX: a) Schematic and b) P-h diagram.

The proposed configurations are studied with and without an IHX to optimize the energy efficiency and keeping the discharge temperature below the limits.

3. Alternative low-GWP refrigerants

Hydrofluorocarbons (HFCs) have been commonly used as refrigerants for HTHPs application, especially HFC-245fa. However, this refrigerant has a GWP value of 858 and can represent a significant contribution to climate change if leaked. According to the IPCC (2005), the annual leakage rate for indirect refrigeration systems contained in machinery rooms can be around 5% of the total refrigerant charge. Therefore, the European Parliament and the Council of the European Union (2014) is gradually limiting the production and use of these chemicals, achieving a maximum allowable quantity of HFCs placed in the market of 21%, compared with the 2015 baseline. Hence, hydrofluoroolefins (HFO), hydrochlorofluoroolefin (HCFO), and natural refrigerants, such as hydrocarbons (HC), illustrate the great potential to replace HFC-245fa as low-GWP refrigerants.

Comprehensive screening analysis of suitable HTHP working fluids was realized by (Frate et al., 2019). They concluded that HCFO-1233zd(E) gives a good compromise between COP and VHC, becoming a potential candidate to replace HFC-245fa. This conclusion is consistent with the results obtained by (Mateu-Royo et al., 2019a), who illustrates that HCFO-1233zd(E) along with HCFO-1224yd(Z) become the most promising low-GWP candidates to replace HFC-245fa.

One requirement for the alternative low-GWP refrigerants in high temperature heating applications is not having notably lower critical temperature than HFC-245fa (154 ºC). This characteristic makes possible similar heating production temperatures than the reference working fluid, operating in subcritical conditions. Based on this requirement, Table 1 presents the selected low-GWP candidates to replace HFC-245fa. All the thermophysical properties displayed in Table 1 are calculated using Engineering Equation Solver (EES) (Klein, 2006).

Table 1. Thermophysical properties of the alternative low-GWP refrigerants and the reference HFC-245fa.

Refrigerant	**Molecular weight (g mol^{-1})**	**T_{crit} (ºC)**	**P_{crit} (MPa)**	**Saturated Vapour density (kg m^{-3})^{a}**	**NBP (ºC)**	**ODP^{b}**	**GWP_{100} ^{b}**	**ASHRAE Std 34 Safety Class^{b}**
HFC-245fa (Ref.)	134.0	154.0	3.65	38.68	15.1	0	858	B1
HC-601	72.2	196.6	3.37	8.93	36.1	0	5	A3
HC-600	58.1	152.0	3.80	22.45	-0.5	0	4	A3

R-514A	139.6	178.0	3.52	22.78	29.1	0[c]	2[c]	B1[c]
HFO-1336mzz(Z)	164.1	171.4	2.90	24.07	33.4	0	2	A1
HCFO-1233zd(E)	130.5	166.5	3.62	30.66	18.3	0.00034	1	A1
HCFO-1224yd(Z)	148.5	155.5	3.33	40.18	14.6	0.00012[d]	<1[d]	A1[d]

[a]At saturated pressure of 75 °C. [b](ASHRAE, 2017). [c](Chemours, 2019). [d](AGC Chemicals, 2017).

R-514A is composed by HFO-1336mzz(Z) and trans-1,2-dichloroethylene (t-DCE). Although HFO-1336mzz(Z) has lower toxicity, the addition of t-DCE produces that R-514A becomes classified with higher toxicity (ASHRAE class B). However, the other alternative candidates present lower toxicity (ASHRAE class A). Regarding the flammability, HFO-1336mzz(Z), R-514A and the HCFOs show no flame propagation (1). The hydrocarbons are included in the highest flammability level (3). Thus, the refrigerants with A1 classification will require lower safety measures than the others, becoming an essential consideration for the final refrigerant selection.

4. Methodology and modeling description

4.1 Methodology

The performance evaluation of this study is calculated based on the methodology presented in Fig. 4. Input parameters as configuration, refrigerant, boundary conditions, along with assumptions, are introduced in an EES computational model. This model includes all the required equations to calculate each configuration and has implemented the thermophysical refrigerant properties database. Moreover, IHX can be included in the simulations in order to model its influence in each configuration proposed. Nevertheless, the IHX requires optimization in order to obtain the maximum system COP without exceeding the discharge temperature limitations. Due to this fact, the Golden Section Search algorithm implemented in EES is used to determine the proper IHX effectiveness. This algorithm is also used in the economizer with parallel compression to maximize the COP with the appropriate sub-cooling degree. Finally, the optimized results are used in the performance analysis.

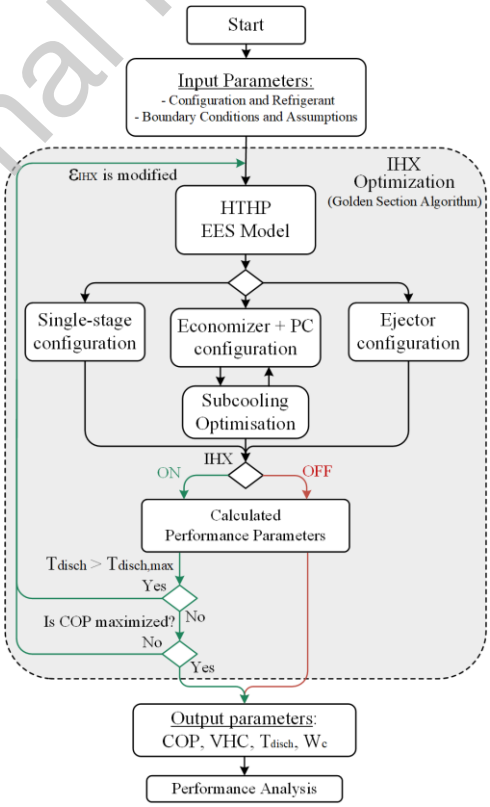

Fig. 4. Methodology flow diagram for the modeling

4.2 Boundary conditions and assumptions

Considering different applications and heat sources, two operating parameters are combined to simulate the typical working conditions: heating production temperature $T_{sink,out}$ and waste heat temperature $T_{source,in}$. The waste heat temperatures selected based on the real application of the outlet temperatures of the water jackets of the cooling engine system (Hoang, 2018). The heat absorbed in the evaporator $\dot{Q}_o$ is considered constant for all the operating conditions. Moreover, an isenthalpic process is considered at the expansion valve. The heat transfer to the surroundings and pressure drops are neglected. Table 2 presents the boundary conditions and assumptions.

Table 2. Assumptions and boundary conditions used in modeling simulation.

Parameter	**Assumed value**
Heating production temperature ($T_{sink,out}$)	110-140 ºC
Waste heat temperature ($T_{source,in}$)	70-90 ºC
Superheat degree	5 K
Sub-cooling degree	2 K
Condenser approach temperature	3 K
Evaporator approach temperature	5 K
Heat sink and source temperature glide	10 K
Electromechanical compressor efficiency (η_{em})	0.95

4.3 Modelling equations

Isentropic and volumetric compressor efficiencies are calculated based on Pierre's correlations for "good" reciprocating compressors (Granryd et al., 1999), using Eq. (1) and (2).

$$\eta_{vol} = k_1 \cdot \left(1 + k_s \cdot \frac{t_{2k} - 18}{100}\right) \cdot \exp(k_2 \cdot \frac{p_1}{p_2}) \quad (1)$$

$$(\frac{\eta_{vol}}{\eta_{is}}) = \left(1 + k_e \cdot \frac{t_{2k} - 18}{100}\right) \cdot \exp(a \cdot \frac{T_1}{T_2} + b) \quad (2)$$

where t_{2k} is the compressor inlet temperature, p_1/p_2 is the pressure ratio, T_1/T_2 the condensation and evaporation absolute temperatures ratio (in Kelvin). The constants values considered are those given by Pierre where k_1, k_s, k_2, k_e, a and b have the values of 1.04, 0.15, -0.07, -0.1, -2.40, and 2.88, respectively. Navarro-Peris et al. (2013) experimentally studied the correlations proposed by Pierre, concluding that these correlations are suitable to describe all types of piston compressors with an error lower than 5%.

The refrigerant mass flow rate is obtained using the Eq. (3) for all the configurations.

$$\dot{m} = \frac{\dot{Q}_o}{(h_{o,out} - h_{o,in})} \quad (3)$$

The volumetric flow rate at the suction line ($\dot{V}_{suc}$) is calculated using Eq. (4) with the refrigerant mass flow rate, the suction density, and the volumetric efficiency.

$$\dot{V}_{suc} = \frac{\dot{m}}{\eta_{vol}\, \rho_{suc}} \quad (4)$$

The discharge temperature T_{disc} is limited to 175 ºC due to the thermal stability of some refrigerants operating at high temperatures (Mateu-Royo et al., 2019a). Hence, the discharge temperature is highly influenced by the IHX effectiveness, ε_{IHX}, and therefore, it is limited.

Then, the enthalpy at the expansion device inlet is calculated considering the IHX heat balance given by the Eq. (5).

$$\varepsilon_{\mathrm{IHX}} = \frac{h_{suc} - h_{o,out}}{h_{k,out} - h_{o,out}} \tag{5}$$

For the economizer with parallel compression configuration, $h_{k,out}$ will be $h_{eco,out}$ and for the ejector configuration, $h_{o,out}$ will be the vapor saturated enthalpy $h_{vap,sat}$ at the liquid receiver conditions.

The compressor power consumption $\dot{W}_C$ is calculated using Eq. (6) as the product of the refrigerant mass flow rate and the compressor isentropic enthalpy difference divided by the isentropic and electromechanical efficiencies.

$$\dot{W}_C = \frac{\dot{m}\,\Delta h_{is,c}}{\eta_{is}\,\eta_{em}} \tag{6}$$

The heating capacity $\dot{Q}_k$ is obtained using Eq. (7) with the product of refrigerant mass flow rate and the inlet and outlet condenser enthalpy difference.

$$\dot{Q}_k = \dot{m}\,(h_{k,in} - h_{k,out}) \tag{7}$$

To compare the influence of the heating capacity and the volumetric flow rate at the suction line, volumetric heating capacity (VHC) is calculated using Eq. (8).

$$VHC = \frac{\dot{Q}_k}{\dot{V}_{suc}} \tag{8}$$

Finally, the Coefficient of Performance (COP) is obtained from the heating capacity and the compressor power consumption, using Eq. (9).

$$COP = \frac{\dot{Q}_k}{\dot{W}_C} \tag{9}$$

For the economizer with parallel compression configuration, the intermediate pressure is calculated considering a temperature approach of 5 K between the liquid economizer outlet and saturated temperature of the expanded liquid fraction. Moreover, the superheat degree of vapor economizer outlet is 5 K. The sub-cooling increment ΔSC is calculated and optimized based on Eq. (10).

$$\Delta SC = T_{k,out} - T_{eco,out} \tag{10}$$

Finally, the energy and mass balance of the different refrigerant mass flow rates is obtained with the Eq. (11) and (12), respectively.

$$\dot{m}_{\mathrm{total}}\, h_{k,out} = \dot{m}\, h_{c,out} + \dot{m}_{PC}\, h_{PC,out} \tag{11}$$

$$\dot{m}_{\mathrm{total}} = \dot{m} + \dot{m}_{PC} \tag{12}$$

Finally, the ejector configuration requires additional modeling equations in order to implement this component in the vapor compression cycle. A constant-pressure mixing model is adopted in this study (Bai et al., 2019; Cui et al., 2020; He et al., 2009), with the following assumptions:

- The mixing process pressure is assumed constant, complying with energy, and momentum conservation.
- The ejector efficiencies are considered with a constant value of 0.5.
- Kinetic energy through the ejector is neglected.
- Adiabatic ejector.

The mass flow rate ratio between the secondary and primary fluid determines the entrainment ratio μ , which is used to evaluate the mass entrainment capacity of the ejector, Eq. (13)

$$\mu = \frac{\dot{m}_s}{\dot{m}_p} \tag{13}$$

The pressure ratio r_p is used to evaluate the pressure rise of the ejector, which is defined by the ratio between the ejector outlet (diffuser) pressure and the secondary inlet fluid pressure, Eq. (14).

$$r_p = \frac{P_I}{P_o} \tag{14}$$

The ejector model is established based on the mass, energy, and momentum conservation in the working process of the ejector components (nozzle, mixing chamber, and diffuser). The inlet velocity of the primary flow is neglected, as previously stated in the assumptions. The isentropic nozzle efficiency η_n is used to obtain the outlet velocity of the primary fluid based on energy conservation, Eq. (15).

$$u_4' = \sqrt{2\,\eta_n\,(h_4 - h_{4,is})} \tag{15}$$

The mixing efficiency η_m considers energy losses caused by the flow friction and two-phase shock in the mixing process. Hence, the mixing velocity u_5 can be obtained from the momentum conservation with Eq. (16).

$$u_5 = \frac{u_4'}{1+\mu}\sqrt{\eta_m} \tag{16}$$

Applying the energy conservation in the diffuser section, inlet and outlet specific enthalpies of the mixed fluid can be calculated using Eq. (17) and (18).

$$h_5 = h_6 - \frac{1}{2}\,(u_5)^2 \tag{17}$$

$$h_6 = \frac{h_4 + \mu\,h_{10}}{1+\mu} \tag{18}$$

The isentropic diffuser efficiency η_d is used to obtain the ideal specific enthalpy at the diffuser outlet with the Eq. (19).

$$h_{6,is} = h_5 + \eta_d(h_6 - h_5) \tag{19}$$

Finally, the intermediate pressure of the ejector outlet P_I can be determined with Eq. (20), and therefore, the ejector outlet state parameters, including temperature, pressure, and quality, can be calculated.

$$P_I = f(h_{6,is}\,, s_{6,is}) \tag{20}$$

5. Results and discussion

This section presents the performance results of each selected configuration altogether with the alternative refrigerant analysis. Finally, the multi-objective analysis illustrates the compromise between COP and VHC of each configuration and refrigerant pair. A single-stage configuration with HFC-245fa as a refrigerant has been used as a reference configuration in this study.

5.1. Configurations performance evaluation

Fig. 5 presents the VHC response of each configuration, operating in different heat sink and source temperatures. As heat source temperature increases, the VHC increases, and therefore, the heating capacity is increasing at constant compressor size. However, a heat sink temperature increase produces the contrary effect, reducing the heating capacity of the installation. The IHX addition improves between 37-44% of the VHC compared to the reference configuration. Hence, the heating capacity of the single-stage cycle can be increased with the addition of this component.

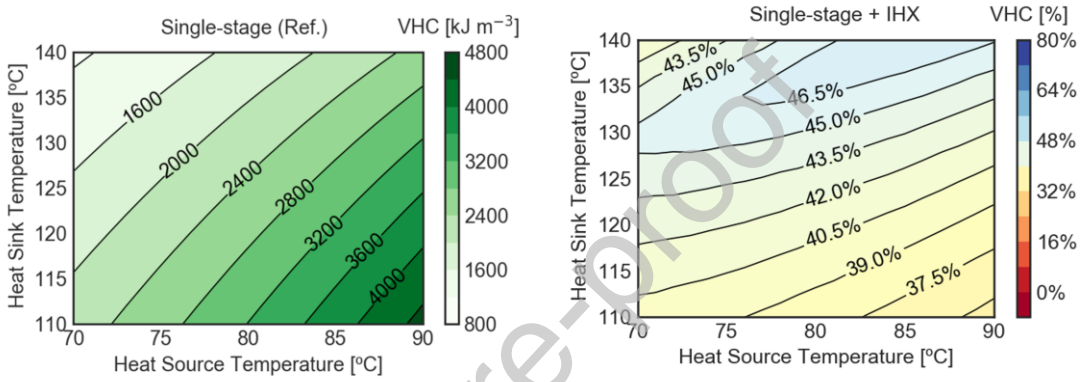

Fig. 5. Volumetric heating capacity of single-stage configuration with and without IHX, using HFC-245fa as working fluid.

The economizer with parallel compression configuration presents a significant VHC increase between 3-38%, as illustrated by Fig. 6. The IHX addition provides a significant VHC increases up to 72.5%, becoming higher with low heat source temperatures. Although the parallel compressor increases the volumetric flow rate, the heating capacity increment becomes more significant, obtaining as a result a substantial VHC increase.

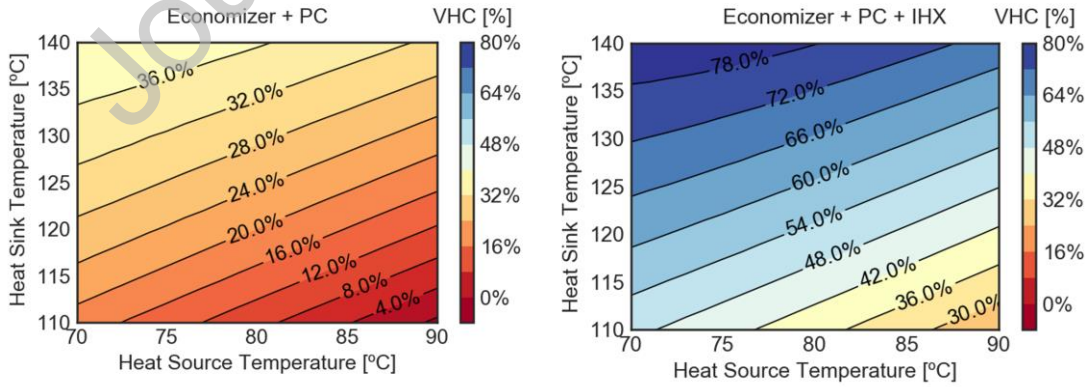

Fig. 6. Volumetric heating capacity of economizer with parallel compressor configuration with and without IHX, using HFC-245fa as working fluid.

Finally, the ejector configuration without IHX shows a light VHC increase, where the IHX addition in this configuration provides a significant VHC augment, as shown in Fig. 7. Whereas the ejector component increases the VHC up to 6%, the ejector configuration with IHX achieves

VHC improvements up to 40%. The major sub-cooling and superheat degree that provides IHX becomes highly beneficial to the ejector configuration from the VHC point of view.

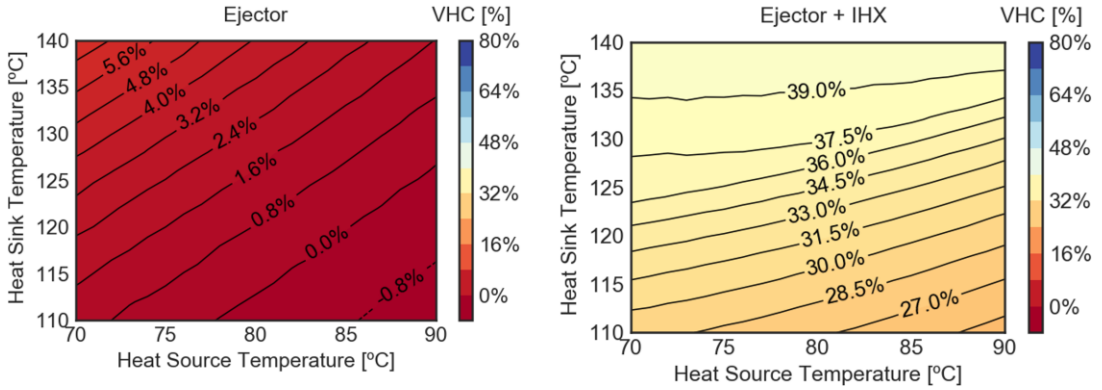

Fig. 7. Volumetric heating capacity of ejector configuration with and without IHX, using HFC-245fa as working fluid

On the other hand, Fig. 8 presents the results of the COP for the six analyzed configurations. In this case, the IHX addition in single-stage configuration increases the COP between 40.5-42%. The IHX effectiveness is limited in order not to exceed the maximum discharge temperatures. Therefore, there is a COP decrease operating at high heat sink temperatures and low heat source temperatures.

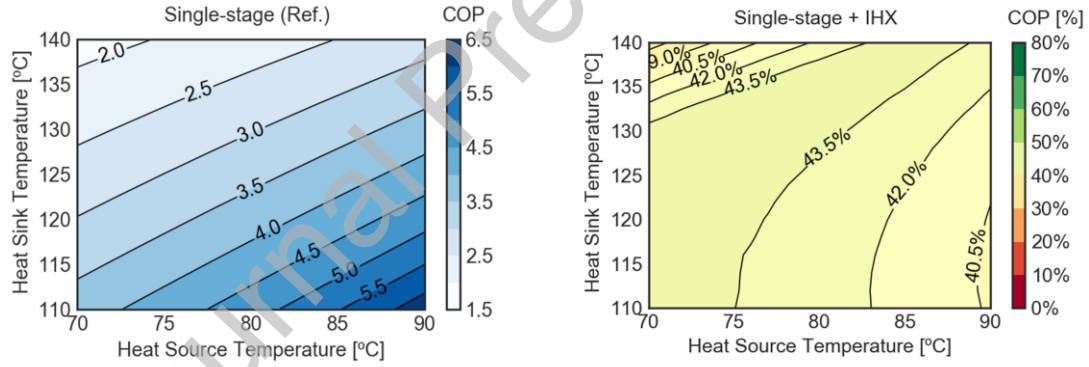

Fig. 8. COP of single-stage configuration with and without IHX, using HFC-245fa as working fluid.

Regarding the economizer with parallel compressor configuration, COP shows an increase of up to 40%, which becomes even higher with the addition of IHX, achieving increment values up to 80%, as shown in Fig. 9. The heating capacity increase in this configuration becomes more significant than the global compressor power consumption, and therefore, a COP increase is appreciated.

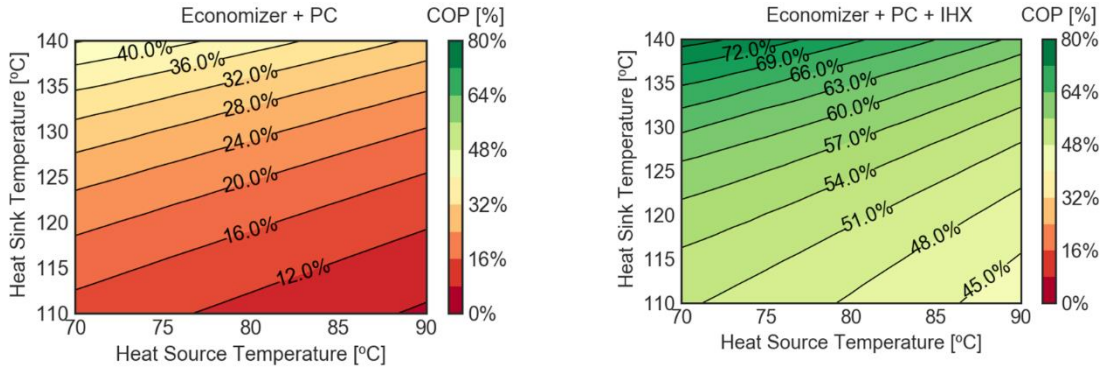

Fig. 9. COP of economizer with parallel compressor configuration with and without IHX, using HFC-245fa as working fluid.

Finally, the ejector configuration shows similar results than the VHC analysis with a slightly COP increase without IHX that reflects a decrease in power consumption compared to the reference, as shown in Fig. 10. With the addition of an IHX, the COP increase becomes up to 36%. Still, the compressor power consumption is higher in this case than the reference configuration at lower heat sink temperatures

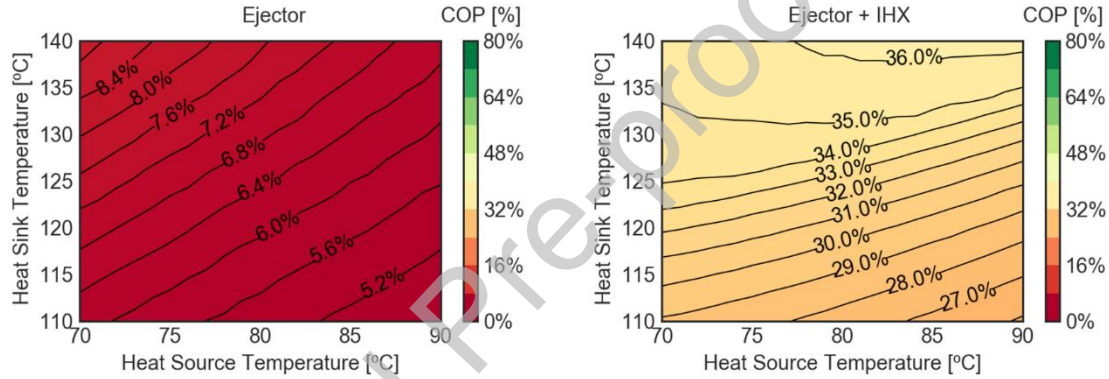

Fig. 10. COP of ejector configuration with and without IHX, using HFC-245fa as working fluid.

Hence, the addition of an IHX in single-stage configuration provides a considerable VHC and COP increase similar to the ejector configuration behaviour. The IHX addition becomes beneficial to the economizer with parallel compression configuration, obtaining the highest COP and VHC values.

5.2 Low-GWP refrigerants assessment

Different alternative low-GWP refrigerants have been considered, and therefore, a proper performance response analysis in the proposed configuration is required. The heat sink temperature is set at 140 ºC, while the heat source temperature remains at 80 ºC. HC-601, HFO-1336mzz(Z), and R-514A require certain superheating degree to ensure the dry compression. This requirement is typically solved with the use of IHX. However, one of the study purposes is illustrate the IHX influence in each configuration and refrigerant. Thus, the configurations are studies with and without IHX, omitting the conditions where dry compression is not ensure.

Single-stage and ejector configurations present similar VHC behavior for each alternative refrigerant, as shown in Fig. 11. HC-601, HFO-1336mzz(Z), and R-514A illustrate a considerable VHC decrease compared to the reference fluid HFC-245fa. This phenomenon is caused by the low suction density that requires greater compressor size to provide the same heating capacity. HCFO-1233zd(E) and HCFO-1224yd(Z) show similar VHC values, and therefore, similar compressor size than HFC-245fa can be used to provide the same heating capacity. HC-600 presents a VHC increase that represents small compressor size requirements, using this refrigerant. However, an economizer with a parallel compressor illustrates an entirely

different response than the other configuration. In this case, all the proposed refrigerants present similar or even higher VHC values than the reference working fluid HFC-245fa.

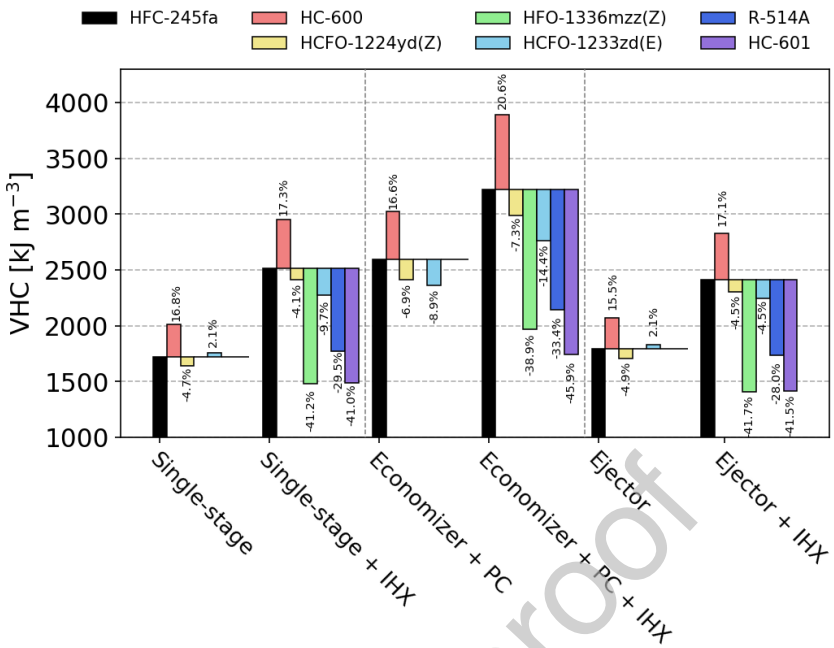

Fig. 11. VHC analysis of alternative low-GWP refrigerants in each configuration at a heat sink temperature of 140 ºC and a heat source temperature of 80 ºC.

On the other hand, the use of alternative low-GWP refrigerants instead of HFC-245fa becomes beneficial from the COP point of view, as shown in Fig. 12. Most of the candidates present considerable COP improvement compared to the reference HFC-245fa. Although HC-601 and R-514A show the lowest VHC values, they provide the highest COP values in most of the proposed configurations, followed by HCFO-1233zd(E). HFO-1336mzz(Z) and HCFO-1224yd(Z) present a slightly COP increase in most of the configurations, whereas HC-600 shows similar or even lower COP values in most of the configurations. Due to the VHC and COP differences in each refrigerant and configuration, a proper multi-objective evaluation is required to illustrate the configuration and refrigerant trade-off between COP and VHC parameters.

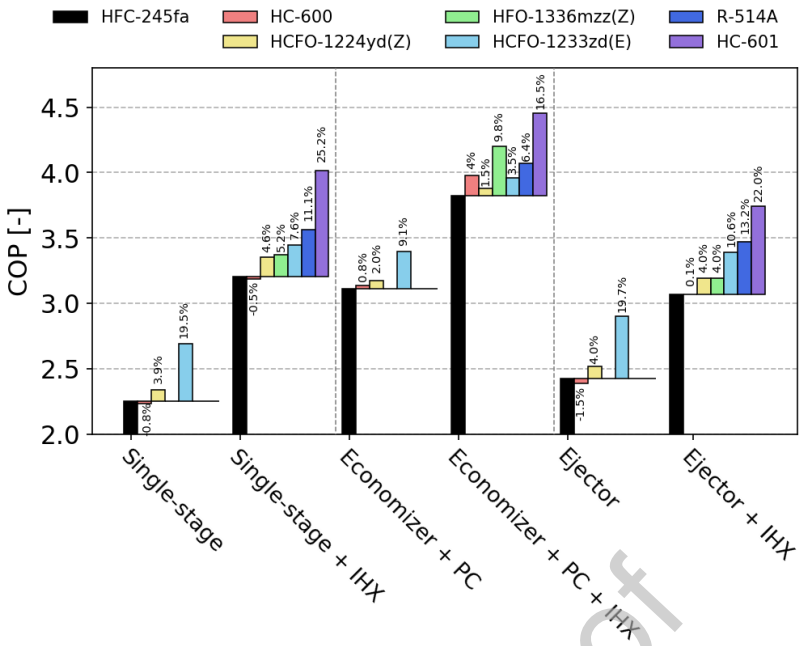

Fig. 12. COP analysis of alternative low-GWP refrigerants in each configuration at a heat sink temperature of 140 ºC and a heat source temperature of 80 ºC.

5.3 Multi-objective comparison

Fig. 13 presents the multi-objective analysis of the proposed configurations and refrigerants compared to a single-stage configuration with HFC-245fa, used as a reference, and the same operating temperatures than the previous section.

This multi-objective evaluation illustrates the proper configuration and refrigerant combination for each application. All the possible combinations provide higher COP values than the reference case. Single-stage and ejector configurations with IHX present similar results in terms of COP and VHC. Without IHX, ejector configurations present benefits than single-stage configuration slightly. Nevertheless, this situation becomes reverse when IHX is activated.

Economizer with parallel compression and IHX presents the highest COP and VHC, and therefore, this configuration becomes promising in high temperature applications with low temperature lifts. The refrigerant selection must consider than the performance difference can vary significantly. Whereas HC-601 provides the highest COP with similar VHC than the reference configuration, whereas HC-600 presents a significant VHC increase, obtaining higher COP than the reference.

As an overall analysis, HC-601, HFO-1336mzz(Z) and R-514A provide the highest COP with a similar or even lower VHC than single-stage cycle with HFC-245fa. Contrary, HC-600 has a significant VHC improvement, providing similar COP than HFC-245fa. Finally, HCFO-1233zd(E) and HCFO-1224yd(Z) become the refrigerants alternative with a compromise between COP and VHC.

Finally, single-stage with IHX becomes easier to implement in practice than economizer with parallel compression and IHX because this configuration only requires one more component. However, the performance and VHC benefits of parallel compression with economizer and IHX can justify the implementation of this configuration in some applications with a proper economic analysis.

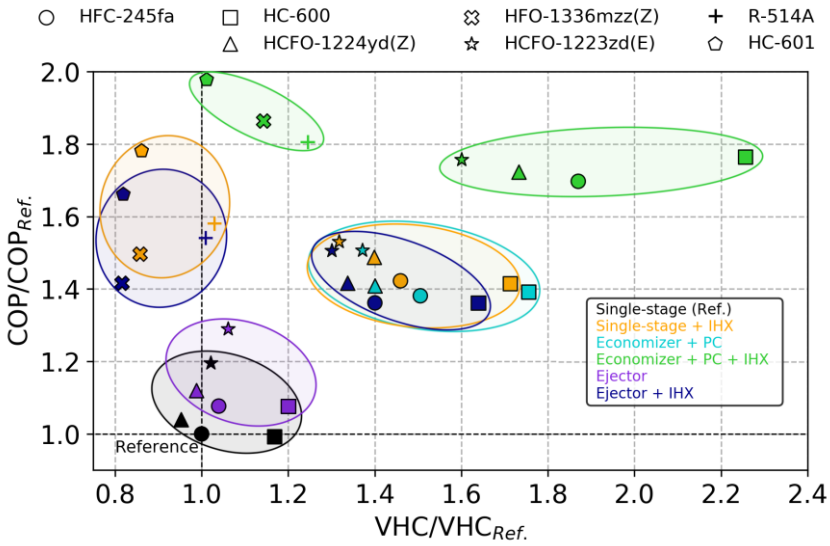

Fig. 13. Multi-objective evaluation of alternative low-GWP refrigerants in each configuration at a heat sink temperature of 140 ºC and a heat source temperature of 80 ºC.

The results obtained in this study are in concordance with other previous. Zhang et al. (2020) illustrate that ejector configurations without IHX provide an experimental COP improvement up to 20% for subcritical systems. Moreover, they suggested that the performance of the ejector configuration can be further improved with the addition of IHX, which is in concordance with the results obtained in this study.

Finally, Fang et al. (2019) concluded that parallel compression with economizer for refrigeration applications increase provides 26-35% higher COP that the conventional system. Moreover, they end that a condensing temperature increases becomes more beneficial for parallel compression with economizer configuration than the conventional. Hence, this configuration will be beneficial for high temperature applications with low temperature lifts between the heat sink and source.

6. Conclusions

This paper provides a comprehensive analysis of ejector and economizer with parallel compression configurations to improve the performance of the single-stage cycle in HTHP applications. Moreover, an IHX has been included in all configurations to extend the analysis and study the influence of this component. Additionally, an alternative low-GWP refrigerant comparison has been carried out in order to evaluate sustainable replacement of the reference working fluid HFC-245fa. The following conclusions can be drawn from the results of this study:

- Ejector and economizer with parallel compression configurations improve the COP compared to the single-stage cycle, with significant VHC differences. Using HFC-245fa, the ejector with IHX configuration presents a COP improvement of up to 36%, with a VHC rise of around 40%. The economizer with parallel compression and IHX configuration achieves the highest COP improvement of up to 72.5% with a considerable VHC increase of approximately 80% compared to the single-stage cycle.

- The addition of an IHX significantly improves the performance in the proposed configurations along with the single-stage cycle. Therefore, this component should be included in high temperature applications to increase the performance efficiency and ensure the dry compression of most of the alternative low-GWP refrigerants.

- HC-601, HFO-1336mzz(Z), and R-514A show the highest COP improvement compared to the reference fluid HFC-245fa along with the maximum VHC decrease. Therefore, greater compressors will be required to provide the same heating capacity than HFC-245fa, and this can produce an increase in the initial cost and volume of the installation. HCFO-1224yd(Z) and HCFO-1233zd(E) present similar VHC values than the reference fluid with a significant COP improvement. Finally, HC-600 improves the VHC, providing the same benefits of COP than HFC-245fa.

- The multi-objective evaluation provides a global comparison of the proposed configurations and refrigerants, ensuring the proper performance trade-off between VHC and COP. Economizer with parallel compression and IHX achieves the highest COP and VHC, whereas single-stage and ejector configurations with IHX become the cycles that balance VHC and COP.

- HC-601 presents the highest COP in each configuration with similar VHC than the single-stage cycle with HFC-245fa. HC-600 provides significant VHC improvements whereas HCFO-1224yd(Z) and HCFO-1233zd(E) result in adequate refrigerants for a compromise between COP and VHC. Depending on the application requirements, different configuration and refrigerant combination can be considered following the multi-objective evaluation.

Declaration of Competing Interest
The authors declare that they have no known competing financial interests or personal relationships that could have appeared to influence the work reported in this paper.

Acknowledgements

The authors acknowledge the Spanish Government for the financial support under projects RTC-2017-6511-3. Furthermore, the authors acknowledge the Universitat Jaume I (Castelló de la Plana, Spain) for the financial support under the projects UJI-B2018-24 and Carlos Mateu-Royo for the funding received through the PhD grant PREDOC/2017/41.

References

AGC Chemicals, 2017. AMOLEA® 1224yd, Technical information. ASAHI Glas. Co. 1–18.

Arpagaus, C., Bless, F., Schiffmann, J., Bertsch, S.S., 2016. Multi-temperature heat pumps: A literature review. Int. J. Refrig. 69, 437–465. https://doi.org/10.1016/j.ijrefrig.2016.05.014

Arpagaus, C., Bless, F., Uhlmann, M., Schiffmann, J., Bertsch, S.S., 2018. High temperature heat pumps: Market overview, state of the art, research status, refrigerants, and application potentials. Energy 152, 985–1010. https://doi.org/10.1016/J.ENERGY.2018.03.166

Arpagaus, C., Kuster, R., Prinzing, M., Bless, F., Uhlmann, M., Büchel, E., Frei, S., Schiffmann, J., Bertsch, S.S., 2019a. High temperature heat pump using HFO and HCFO refrigerants – system design and experimental results, in: Minea, V., IS Event Solutions (Eds.), Refrigeration Science and Technology Proceedings. 25th IIR International Congress of Refrigeration. International Institute of Refrigeration IIR Institut International du Froid IIF, Montreal (Canada), pp. 4239–4247. https://doi.org/10.18462/iir.icr.2019.0242

Arpagaus, C., Prinzing, M., Kuster, R., Stefan S. Bertsch, 2019b. High temperature heat pumps - Theoretical study on low GWP HFO and HCFO refrigerants. 25th IIR Int. Congr. Refrig. (ICR 2019). Montréal, Québec, Canada.

ASHRAE, 2017. ASHRAE Handbook Fundamentals. Am. Soc. Heating, Refrig. Air-Conditioning Eng.

Bai, T., Yan, G., Yu, J., 2019. Thermodynamic assessment of a condenser outlet split ejector-based high temperature heat pump cycle using various low GWP refrigerants. Energy 179, 850–862. https://doi.org/10.1016/J.ENERGY.2019.04.191

Bergamini, R., Jensen, J.K., Elmegaard, B., 2019. Thermodynamic competitiveness of high temperature vapor compression heat pumps for boiler substitution. Energy 182, 110–121. https://doi.org/10.1016/J.ENERGY.2019.05.187

Chemours, 2019. Opteon™ XP30 (R-514A), Technical information 1–16.

Cooper, S.J., Hammond, G.P., Hewitt, N., Norman, J.B., Tassou, S.A., Youssef, W., 2019. Energy saving potential of high temperature heat pumps in the UK Food and Drink sector. Energy Procedia 161, 142–149. https://doi.org/10.1016/J.EGYPRO.2019.02.073

Cui, Z., Qian, S., Yu, J., 2020. Performance assessment of an ejector enhanced dual temperature refrigeration cycle for domestic refrigerator application. Appl. Therm. Eng. https://doi.org/10.1016/j.applthermaleng.2019.114826

Fang, Z., Fan, C., Yan, G., Yu, J., 2019. Performance evaluation of a modified refrigeration cycle with parallel compression for refrigerator-freezer applications. Energy 188, 116093. https://doi.org/https://doi.org/10.1016/j.energy.2019.116093

Frate, G.F., Ferrari, L., Desideri, U., 2019. Analysis of suitability ranges of high temperature heat pump working fluids. Appl. Therm. Eng. 150, 628–640. https://doi.org/10.1016/J.APPLTHERMALENG.2019.01.034

Granryd, E., Ekroth, I., Lundqvist, P., Melinder, A., Palm, B., Rohlin, P., 1999. Refrigeration Engineering. K. Tek. Högskolan.

He, S., Li, Y., Wang, R.Z., 2009. Progress of mathematical modeling on ejectors. Renew. Sustain. Energy Rev. 13, 1760–1780. https://doi.org/10.1016/J.RSER.2008.09.032

Hoang, A.T., 2018. Waste heat recovery from diesel engines based on Organic Rankine Cycle. Appl. Energy 231, 138–166. https://doi.org/10.1016/J.APENERGY.2018.09.022

IPCC, 2005. IPCC/TEAP special report on safeguarding the ozone layer and the global climate system: Issues related to hydrofluorocarbons and perfluorocarbons. Cambridge Publ. Intergov. Panel Clim. Chang. [by] Cambridge Univ. Press.

Klein, S., 2006. Engineering Equation Solver (EES) V10.2. Fchart software, Madison, USA www.fchart.com.

Kosmadakis, G., 2019. Estimating the potential of industrial (high-temperature) heat pumps for exploiting waste heat in EU industries. Appl. Therm. Eng. 156, 287–298. https://doi.org/10.1016/J.APPLTHERMALENG.2019.04.082

Luo, B., Zou, P., 2019. Performance analysis of different single stage advanced vapor compression cycles and refrigerants for high temperature heat pumps. Int. J. Refrig. 104, 246–258. https://doi.org/https://doi.org/10.1016/j.ijrefrig.2019.05.024

Mateu-Royo, C., Navarro-Esbrí, J., Mota-Babiloni, A., Amat-Albuixech, M., Molés, F., 2019a. Thermodynamic analysis of low GWP alternatives to HFC-245fa in high-temperature heat

pumps: HCFO-1224yd(Z), HCFO-1233zd(E) and HFO-1336mzz(Z). Appl. Therm. Eng. https://doi.org/10.1016/j.applthermaleng.2019.02.047

Mateu-Royo, C., Navarro-Esbrí, J., Mota-Babiloni, A., Amat-Albuixech, M., Molés, F., 2018. Theoretical evaluation of different high-temperature heat pump configurations for low-grade waste heat recovery. Int. J. Refrig. https://doi.org/10.1016/j.ijrefrig.2018.04.017

Mateu-Royo, C., Navarro-Esbrí, J., Mota-Babiloni, A., Molés, F., Amat-Albuixech, M., 2019b. Experimental exergy and energy analysis of a novel high-temperature heat pump with scroll compressor for waste heat recovery. Appl. Energy 253, 113504. https://doi.org/10.1016/j.apenergy.2019.113504

Mohammadi, K., Powell, K., 2020. Thermodynamic and economic analysis of different cogeneration and trigeneration systems based on carbon dioxide vapor compression refrigeration systems. Appl. Therm. Eng. 164, 114503. https://doi.org/https://doi.org/10.1016/j.applthermaleng.2019.114503

Mota-Babiloni, A., Mateu-Royo, C., Navarro-Esbrí, J., Molés, F., Amat-Albuixech, M., Barragán-Cervera, Á., 2018. Optimization of high-temperature heat pump cascades with internal heat exchangers using refrigerants with low global warming potential. Energy 165, 1248–1258. https://doi.org/10.1016/j.energy.2018.09.188

Navarro-Peris, E., Corberán, J.M., Falco, L., Martínez-Galván, I.O., 2013. New non-dimensional performance parameters for the characterization of refrigeration compressors. Int. J. Refrig. 36, 1951–1964. https://doi.org/https://doi.org/10.1016/j.ijrefrig.2013.07.007

Pérez-García, V., Rodríguez-Muñoz, J.L., Ramírez-Minguela, J.J., Belman-Flores, J.M., Méndez-Díaz, S., 2016. Comparative analysis of energy improvements in single transcritical cycle in refrigeration mode. Appl. Therm. Eng. 99, 866–872. https://doi.org/https://doi.org/10.1016/j.applthermaleng.2016.01.092

Rodríguez-Muñoz, J.L., Pérez-García, V., Belman-Flores, J.M., Ituna-Yudonago, J.F., Gallegos-Muñoz, A., 2018. Energy and exergy performance of the IHX position in ejector expansion refrigeration systems. Int. J. Refrig. 93, 122–131. https://doi.org/https://doi.org/10.1016/j.ijrefrig.2018.06.017

Sun, Z., Li, J., Liang, Y., Sun, H., Liu, S., Yang, L., Wang, C., Dai, B., 2020. Performance assessment of CO2 supermarket refrigeration system in different climate zones of China. Energy Convers. Manag. 208, 112572. https://doi.org/https://doi.org/10.1016/j.enconman.2020.112572

Tello-Oquendo, F.M., Navarro-Peris, E., Barceló-Ruescas, F., Gonzálvez-Maciá, J., 2019. Semi-empirical model of scroll compressors and its extension to describe vapor-injection compressors. Model description and experimental validation. Int. J. Refrig. 106, 308–326. https://doi.org/https://doi.org/10.1016/j.ijrefrig.2019.06.031

The European Parliament and the Council of the European Union, 2014. Regulation (EU) No 517/2014 of the European Parliament and the Council of 16 April 2014 on fluorinated greenhouse gases and repealing Regulation (EC). No 842/2006. Off. J. Eur. Union 150, 195–230.

Urbanucci, L., Bruno, J.C., Testi, D., 2019. Thermodynamic and economic analysis of the integration of high-temperature heat pumps in trigeneration systems. Appl. Energy 238, 516–533. https://doi.org/10.1016/J.APENERGY.2019.01.115

Zhang, Z., Feng, X., Tian, D., Yang, J., Chang, L., 2020. Progress in ejector-expansion vapor compression refrigeration and heat pump systems. Energy Convers. Manag. 207, 112529. https://doi.org/https://doi.org/10.1016/j.enconman.2020.112529